Accepted Manuscript

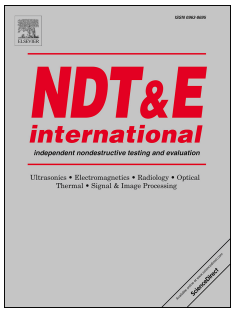

Multiple type defect detection in pipe by Helmholtz electromagnetic array probe

Jiuhao Ge, Wei Li, Guoming Chen, Xiaokang Yin, Xinan Yuan, Weichao Yang, Jian Liu, Yuxi Chen

PII: S0963-8695(16)30131-1

DOI: 10.1016/j.ndteint.2017.07.001

Reference: JNDT 1879

To appear in: *NDT and E International*

Received Date: 20 October 2016

Revised Date: 23 May 2017

Accepted Date: 4 July 2017

Please cite this article as: Ge J, Li W, Chen G, Yin X, Yuan X, Yang W, Liu J, Chen Y, Multiple type defect detection in pipe by Helmholtz electromagnetic array probe, *NDT and E International* (2017), doi: 10.1016/j.ndteint.2017.07.001.

Multiple Type Defect Detection in Pipe by Helmholtz Electromagnetic Array Probe

Jiuhao Ge; Wei Li[1]; Guoming Chen; Xiaokang Yin; Xinan Yuan; Weichao Yang; Jian Liu; Yuxi Chen;
(Centre for Offshore Engineering and Safety Technology, China University of Petroleum, Qingdao, China)

Abstract: Non-destructive testing plays a key role in the detection of pipe. In this paper, a Helmholtz electromagnetic array probe, with the advantages of multiple type defect detection, quantification, non-contacting and good applicability on ferromagnetic pipe, is presented. A designed structure, containing a high precision tunnel magneto-resistive (TMR) array sensor, is used to scan the full circumference of pipe in a single pass. In the experiments, multiple types of detects, e.g. hole, axial crack and circumferential crack are detected through the probe. The profile of the defects can be inferred approximately. Moreover, the pipe of different radius are inspected showing that the radius of pipe has little effect on the detection sensitivity if the Helmholtz Probe proposed in this paper is used.

Keywords: Helmholtz coil; Array Probe; Multiple Type Defect Detection; Pipe; Electromagnetic method;

1 introduction

Ferromagnetic pipe such as oil well tubing, drill pipes and risers *et al*. are widely used in the oil industry [1]. Subjected to variable loads and complex environment, pipe frequently suffers from stress corrosion crack, fatigue crack, corrosion and deformation, all of which will give rise to catastrophic accident [2]. Pipe can be inspected, using Magnetic Flux Leakage (MFL), Ultrasound Test (UT), Magnetic Particle Inspection (MPI) and Eddy Current (EC) methods [3-4]. The MFL technique has been proved to be an effective way to detect cracks on pipe through in-line inspections. However, the inspected pipe have to achieve complete magnetic saturation condition and the direction of magnetization should be varied depending on the types of metal loss [5-7]. Alternating

Flux Leakage testing was proposed to achieve fast detection [7-8]. However, the detection of axial narrow and long defects is still restricted [9]. The MPI technique is also a preferred technique for crack detection historically. However, due to its requirement for the surface cleaning before the inspection, its field use is costly when one considers the standby time of other trades when the MPI inspection and documentation is in progress [2].

In the case of UT, liquid couplant is usually needed between the device and the pipe surface through the traditional UT devices [3,10-12]. Moreover, manual operation requires careful attention by experienced technicians and it is difficult to locate the position and invert the sizes of defects [11-12]. In recent years, Electromagnetic Acoustic Transducer (EMAT) is becoming increasingly popular due to its non-contact nature [13-14]. Generating ultrasonic waves directly into the testing piece instead of coupling through the transducer, EMAT can be applied where surface contact is not possible or desirable [15-16]. However, EMAT transducers typically produce raw signals of lower power than piezoelectric transducers. As a result, more sophisticated signal processing techniques are needed to isolate signals from noise [17]. Guided Wave Testing (GWT) employs the ultrasonic guided by the inspected structure and offers the possibility of rapid screening over long lengths of the pipelines for the detection of corrosion and other defect [18-19]. Thus, it has attracted much attention in pipelines corrosion monitoring during the past few decades

[1] Corresponding author: Wei Li
Email: ronald8044@163.com, Address: No.66 Changjiang road, Huangdao, Qingdao, China

[19-22]. Similar to the traditional UT, the interpretation of the data of GWT is highly operator dependent; in addition, it failed to find small pitting defect [22-23].

For EC method, using the non-uniform induced field, it cannot make quantitative rapid assessment of crack sizes; meanwhile, it is excessively sensitive to the lift-off distance [25-26]. In contrast, a uniform induced current field would have the advantages of non-contact detection, being insensitive to lift-off and complete mathematical model which can achieve quantitative recognition of defect sizes [27-29]. Using a uniform field, an ACFM system was employed to detect the surface-breaking RCF defects at high inspection speeds under laboratory conditions [30]. A rotating uniform current field induced by a U-shaped orthogonal inducer was proposed in RACFM technology to detect arbitrary orientation crack [31]. However, it was inadequate to scan the full circumference of pipe string simultaneously in a single pass [32-33]. Moreover, the variation of lift-off distance will cause detection error when the probe scans on the camber of pipe [33].

According to defect type to be found, inspection tools may vary, as the aspect ratio of a given feature, i.e. the length to width has an effect on the sensitivity of the tool used [9]. It is inefficient to carry out the repetitive scans. Thus, a more sensitive and reliable NDE technique that can achieve full circumferential detection and quantification for multiple type defect in pipe is needed.

Helmholtz coil is a widely used device, which is often used to induce uniform magnetic field or form standard magnetic field [34-35]. Jianping Peng and Kongjing Li *et al.* used uniform magnetic field (UMF) excited by Helmholtz coils to investigate the eddy current pulsed thermography for rolling contact fatigue and state detection of bond wires in IGBT modules [36-37]. A Helmholtz-coil-type eddy current probe was also presented to detect longitudinal cracks less than 50um in heat-exchanger copper tubes using an HTS-SQUID gradiometer [38]. B Wu *et al*. proposed a MFL sensor excited by a direct current Helmholtz-coil to carry out steel wire rope inspection [39].

From the literature above, B Wu and Hatsukade Y [38-39] respectively used the Helmholtz coil excited by direct current and alternating current to study the detectability of steel wire rope and copper tubes. Nevertheless, according to the Faraday law of electromagnetic induction, if a pipe, which is mainly made of ferromagnetic materials, locates in the center of the Helmholtz coil excited by alternating current, not only uniform magnetic field but also uniform current field will be induced on the surface of the pipe. These orthogonal fields may have prospect to detect and size multiple type defect on the surface of pipe.

The aim of this paper is to propose a Helmholtz-coil-type electromagnetic array probe excited by alternating current for detecting of multiple type defect on the surface of pipe in petroleum industry. This paper is organized as follows: In section 2, the theoretical equations of Helmholtz coil will be presented and then the model of Helmholtz-coil-type probe will be built by 3-dimensional finite element method; meanwhile, axial and circumferential cracks in pipe will be inspected to test the detectability of the Helmholtz-coil probe. Furthermore, the influence of coil radius and distance will be analyzed. In section 3, the structure of Helmholtz-coil array probe will be presented. In section 4, to actually test the detectability of the probe, defects of hole, axial crack and circumferential crack will be detected in experiments. ϕ 65 and ϕ 75 pipes with the same axial cracks will also be inspected to study the sensitivity of the probe to pipe with different radius.

2 Physics of the Helmholtz-coil

2.1 Magnetic field induced by Helmholtz coil

The problem of a delta-function coil encircling an infinitely long rod has been researched by DODD and DEEDS [38]. The differential equation for the vector potential *R(r,z)* in an isotropic, linear, and inhomogeneous medium due to an applied alternating current *I* is:

$$\frac{\partial^2 R}{\partial r^2}+\left(\frac{1}{r}\right)\frac{\partial R}{\partial r}+\frac{\partial^2 R}{\partial z^2}-\frac{R}{r^2}=0 \text{ (in air)} \tag{1}$$

$$\frac{\partial^2 R}{\partial r^2}+\left(\frac{1}{r}\right)\frac{\partial R}{\partial r}+\frac{\partial^2 R}{\partial z^2}-\frac{R}{r^2}-j\omega\sigma_i R=0 \text{ (in conductor)} \tag{2}$$

Setting $R(r,z)=R(r)\,\mathrm{Z}(z)$ and dividing by $R(r)\,\mathrm{Z}(z)$ gives:

$$\frac{1}{R(r)}\frac{\partial^2 R(r)}{\partial r^2}+\frac{1}{rR(r)}\frac{\partial R(r)}{\partial r}+\frac{1}{Z(z)}\frac{\partial^2 Z(z)}{\partial Z^2}-\frac{1}{r^2}-j\omega\mu\sigma=0 \text{ (in conductor)} \tag{3}$$

Assuming the separation constant to be negative:

$$\frac{1}{Z(\mathrm{z})}\frac{\partial^2 \mathrm{Z(z)}}{\partial z}=\text{"}contrast\text{"}=-\alpha^2 \tag{4}$$

And Eq. (3) becomes:

$$\frac{r^2\partial^2 R(r)}{\partial r^2}+r\frac{\partial R(r)}{\partial r}-\left[(\alpha^2+j\omega\mu\sigma)r^2+1\right]R(r)=0 \tag{5}$$

The solution to Eq. (5) in terms of modified Bessel functions is:

$$R(r)=CI_1\left[(\alpha^2+j\omega\mu\sigma)^{1/2}r\right]+DK_1[(\alpha^2+j\omega\mu\sigma)^{1/2}r] \tag{6}$$

$$Z(z)=E\sin\alpha(z-z_0)+F\cos\alpha(z-z_0) \tag{7}$$

The magnetic field and current field will be axially and circumferential induced on the surface of pipe. The fields induced by the encircling coil with finite cross section is relatively constant over a large outer portion of the pipe and rapidly decreases toward the center of the pipe [40].

If two coils with a distance of coil radius, which is called Helmholtz coil as shown in Figure.1, encircle a pipe, the different equations for the vector potential in pipe and air are [41]:

$$R(r,z)^a=R(r,z)_1^a+R(r,z)_2^a \text{ (in conductor)} \tag{8}$$

$$R(r,z)_1^a=\frac{\mu I}{\pi}\int_0^\infty\frac{r_0}{R_1}\frac{K_1(\alpha r_0)I_1(\alpha_1 r)\cos\left(z-\frac{r_0}{2}\right)}{\left[\alpha I_1(\alpha_1 R_1)K_0(\alpha R_1)+\alpha_1 I_0(\alpha_1 R_1)K_1(\alpha R_1)\right]}d\alpha \tag{9}$$

$$R(r,z)_2^a=\frac{\mu I}{\pi}\int_0^\infty\frac{r_0}{R_1}\frac{K_1(\alpha r_0)I_1(\alpha_1 r)\cos\left(z+\frac{r_0}{2}\right)}{\left[\alpha I_1(\alpha_1 R_1)K_0(\alpha R_1)+\alpha_1 I_0(\alpha_1 R_1)K_1(\alpha R_1)\right]}d\alpha \tag{10}$$

$$R(r,z)^b=R(r,z)_1^b+R(r,z)_2^b \text{ (in air)} \tag{11}$$

$$R(r,z)_1^b=\frac{\mu I}{\pi}\int_0^\infty r_0K_1(\alpha r_0)\left\{I_1(\alpha r)+\left[\frac{I_1(\alpha_1 R_1)}{R_1K_1(\alpha R_1)[\alpha I_1(\alpha_1 R_1)K_0(\alpha R_1)+\alpha_1 I_0(\alpha_1 R_1)K_1(\alpha R_1)]}-\frac{I_1(\alpha R_1)}{K_1(\alpha R_1)}\right]K_1(\alpha r)\right\}\cos\alpha(z-\tfrac{r_0}{2})d\alpha \tag{12}$$

$$R(r,z)_1^b=\frac{\mu I}{\pi}\int_0^\infty r_0K_1(\alpha r_0)\left\{I_1(\alpha r)+\left[\frac{I_1(\alpha_1 R_1)}{R_1K_1(\alpha R_1)[\alpha I_1(\alpha_1 R_1)K_0(\alpha R_1)+\alpha_1 I_0(\alpha_1 R_1)K_1(\alpha R_1)]}-\frac{I_1(\alpha R_1)}{K_1(\alpha R_1)}\right]K_1(\alpha r)\right\}\cos\alpha(z+\tfrac{r_0}{2})d\alpha \tag{13}$$

Where

$$\frac{1}{z}K_1(\mathrm{z})+\frac{d}{dz}K_1(z)=-K_0(z) \tag{14}$$

$$\frac{1}{z}I_1(z)+\frac{d}{dz}I_1(z)=-I_0(z) \tag{15}$$

$$\alpha_1=(\alpha^2+j\omega\mu\sigma_1) \tag{16}$$

The superposition vector potential of two coils will enlarge the area of uniform electromagnetic field; meanwhile, the orthogonal induced magnetic field and induced current field will have prospect to detect and size multiple type defect in pipe.

2.2 Defect detectability of Helmholtz-coil-type probe

A Helmholtz-coil-type electromagnetic probe presented in this paper consisted of a sensor array and two coaxial excitation coils whose distance was the radius of the coils. An alternating excitation was applied to the Helmholtz coil. The finite element method (FEM) was used to build this Helmholtz-coil-type electromagnetic probe through the COMSOL software, as shown in Figure.2. The model was built by "frequency domain analysis" and "magnetic field domain" integrated in the COMSOL [27, 43]. To save calculation time, the "Impedance Boundary Condition" provided by COMSOL was applied on the surface of specimen, providing a boundary condition that is useful for boundaries where the electromagnetic field penetrates only a short distance outside the boundary [44]. It is a valid approximation if the skin depth is small compared to the size of the conductor or crack; it can reduce the mesh quantity and calculation time. The assuming equation can be defined by:

$$\sqrt{\frac{\mu_0\mu_r}{\varepsilon_0\varepsilon_r-j\sigma/\omega}}n\times H+E-(n\cdot E)n=(n\cdot E_s)n-E_s \tag{17}$$

μ_0 --space permeability, μ_r --relative permeability, ε_r --relative permittivity, ε_0 -- space permittivity, σ --electrical conductivity, E --electric field intensity, E_s --source electric field, n --normal vector of conductor.

The dimensions of the model are shown in Table.1 and the characteristic parameters are shown in Table.2. The electromagnetic field induced on the surface of specimen without crack is shown in Figure.3, where the axial black arrows are induced magnetic field and circumferential red arrows are induced current.

Table.1 Sizes of model

Model	Diameter/mm	Length/mm	Distance/mm
String(D/d)	65/45	300	-
Excitation coil(D1)	80	-	40
Air	-	-	-

Table.2 Characteristic parameters of model

Coil diameter/mm	Number of turns	String material	Current/A	Permeability	Conductivity/ S/m	Frequency/Hz
0.15	1000	Carbon steel	0.5	4000	1.12e7	1000

Then, the induced magnetic density and electric current density distributions are shown in Figure.4. It can be seen that the uniform electric current field and magnetic field present on the surface of pipe.

Axial and circumferential cracks were examined to test the detectability of Helmholtz electromagnetic probe and the parameters of cracks are shown in Table.3. The probe was moved along the axial direction of pipe to simulate the scanning process along a pipe. The response magnetic field was measured at a 1mm lift-off distance. The absolute value of axial component

magnetic flux density B_z and radial component magnetic flux density B_y were measured as characteristic signals, as shown in Figure.5 and Figure.6. From the data in figures we can see that both of the cracks can be detected. When the axial crack is detected, there is a dip in B_z and a 'm' in B_y. When the circumferential crack is detected, there is a peak in B_z and a 'm' in B_y. The dip or peak of B_z locates at the center of the cracks. The peaks of B_y exactly locate at both the ends of the cracks, which can represent the length or width of the cracks.

Table.3 Crack parameters

Crack	X position/mm	Length/mm	Width/mm	Depth/mm
Axial crack	20	20	1	6
Circumferential crack	20	20	1	6

The axial crack result can be explained by the fact that when the axial crack is detected, the induced current is perpendicular to crack and the induced current will flow down the crack and around the ends of the crack, as shown in Figure.7a. On the contrary, the axial crack cannot disturb the magnetic field which is parallel to it [45].

For the circumferential crack, the induced current is parallel to it; however, the magnetic field is perpendicular to it. So the magnetic flux will leak around the circumferential crack as shown in Figure.7b.

In summary, the theory of current perturbation and magnetic flux leakage around defect can be shown in Figure.8. The current perturbation effect makes up the restriction of magnetic flux leakage effect for axial crack detection. Using the superposition effect of current perturbation and magnetic flux leakage, multiple type of defect in pipe can be detected.

2.3 Influence of Radius of Helmholtz-coil on the measured signal

The Helmholtz coil has the advantage of uniform magnetic field. Figure.9 shows the magnetic field distribution along the axial and the radial direction of the Helmholtz coil without pipe. It can be seen from the figures that the magnetic field along the axial direction between the two coils is uniform and the magnetic field along the radial direction between 1/2 radius of the Helmholtz coils is also uniform. Normally, pipe have different radius according to the different application, which will influence the structure of inspection tools. A useful implication of Helmholtz coil may be that the induced magnetic field and current field in pipe may not change with the variation of pipe radius by the virtue of uniform magnetic field. In other words, the Helmholtz probe is insensitive to the radius variation of pipe.

To verify the assumption above, the radius of Helmholtz coil model were changed from 40 to 90mm, with other parameters remain invariant. The sensitivity of B_z was obtained using the formula expressed in formula (10):

$$\eta = \frac{|\Delta B_z|}{B_0} \tag{22}$$

Where:

$$\Delta B_z = B_{z,peak/dip} - B_0 \tag{23}$$

$B_{z,peak/dip}$ --the peak or dip value of B_z , B_0 --the value of B_z without crack

The relationship between detection sensitivity of the axial and the circumferential crack and the variation of D_1/D (diameter of the Helmholtz coil D_1 divide diameter of the pipe D) is shown in Figure.10.

As can be seen from Figure.10, with parameter D_1/D increasing, the detection sensitivities of the axial and the circumferential cracks both decrease. However, when the D_1/D changes in the range of 1.85~2.77, the detection sensitivities of the axial and circumferential cracks decrease with the maximum variation rate of 4.6% and 7.7% respectively. It indicates that Helmholtz probe is insensitive to the radius of pipe in some extent.

2.4 Influence of coil distances on detection sensitivity

Here, the influence of coil distances on detection sensitivity was researched. Axial and circumferential cracks (length*width=20*1 mm) with the depth of 2mm, 4mm, 6mm, 8mm were detected and the results are shown in Figure.11.

From Figure.11, it is observed that detection sensitivity linearly increases with crack depth. From Figure.11a it is also observed that, detection sensitivity of axial crack in different coil distance gradually increases up to 40mm and then decreases. In addition, from Figure.11b it is observed that, the detection sensitivity of circumferential crack increases up to 20mm and then decreases; meanwhile, the detection sensitivity of 20mm and 40mm coil distance are almost same.

In consequence, the coil distance equaling to the coil radius can obtain the most sensitivity result in comprehensive consideration.

3 Design of Helmholtz-coil-type electromagnetic probe

3.1 Structure of the Helmholtz probe

The structure of the Helmholtz probe is shown in Figure.12. The radius of the Helmholtz-coil was 40mm and the excitation coils were wound on the polymer frame. The detecting sensors were equally-spaced installed in the polymer frame. The supports were used to fix the probe and can be moved to keep the sensor array having a constant lift-off distance of 1mm to the pipe surface of different radius. The extension-type tape was used to fix the sensor array.

3.2 TMR-based sensor array

Tunnel magneto resistive (TMR) element is a new sensitive magnetic sensor which has superior performances over GMR, but at present is rarely used for NDT application [38]. A commercial TMR device, in which four elements forms a Wheatstone bridge, was employed in our probe. The parameters of the TMR provided by the manufacturer were listed in Table.4. The TMR sensor and electronic circuits that contained signal amplification module and filter module were fixed in the PCB, as shown in Figure.13.

A sensor array containing TMR was employed in the Helmholtz-coil-type electromagnetic probe to achieve rapid full circumferential detection. In previous work [1], an acceptable maximum detection range of each detection sensor was ±10 degrees along the circumference by feed-through ACFM probe. Considering the space of Helmholtz-coil-type electromagnetic probe and actual manufacturing difficulty, a 24 equal-spaced sensor array was selected.

Table.4 Parameters of the TMR sensor

Name	Type	Linear range(Oe)	Sensitivity(mV/V/Oe)	Non-linearity(%FS)	Hysteresis(Oe)	Supply voltage(v)
TMR	MMLP57F	±30	4.9	1	0.1	1

4 Experiments

4.1 System set up

A Helmholtz-coil-type electromagnetic detection system was built and the schematic diagram is Figure.14. The excitation source produced an alternating current signal with frequency of 1kHz and magnitude of 0.5A. The turns of the coil were 1000 in total. The current was transferred to the excitation coil through the power amplifiers. The detecting sensor array measured the magnetic

field and translated it into electric signals. The signals were amplified and filtered in the signal processing module. And then, the signals were converted into digital signals by an A/D convertor and sent to PC for signal processing. A detection software was developed to achieve defects recognition. B_z and B_y signals were shown in the display screen of computer. The Helmholtz probe was fixed in an axial scan table, the pipe was coaxially moved through the probe at a speed of 10mm/s. The experimental setup is shown in Figure.15.

4.2 Detectability testing

To actually test the detectability of Helmholtz-coil-type electromagnetic probe, axial crack, circumferential crack and hole, which were machined in steel pipe by Electrical Discharge machining (EDM), were detected. The parameters of pipe and defects are listed in Table.5 and shown in Figure.16.

Table.5 Parameters of pipe strings and defects

Name	Outside Diameter/mm	Thickness/mm	Length/mm	Width/mm	Depth/mm
Pipe	65	10	300	-	-
Hole	-	-	30	20	5
Axial crack	-	-	30	0.8	4
Circumferential crack	-	-	30	0.8	4

The B_z signal of defect is shown in Figure.17 and the detection sensitivity of Helmholtz probe to different defects is shown in Table.6. It is apparent from those results that all of the defects in pipes could be detected. It indicates that the Helmholtz probe owns the detectability of crack and corrosion hole by the virtue of the superposition effect of the current perturbation and magnetic flux leakage.

Table.6 Detection sensitivity of Helmholtz probe to different defects

Defect type	Sensitivity/%
Axial crack	13.2%
Circumferential crack	12.6%
Hole	14.7%

Then, we obtained the surface scan results of the axial crack, circumferential crack and hole through the sensor array, as shown in Figure.18. As can be seen from the figures, the profile of the defects can be inferred approximately.

4.3 Detection on pipe string of different D_1/D

Usually, the structure of inspection tool need to be changed to detect pipe with different radius. Here, steel pipe with diameters of 65mm (D_1/D=1.23) and 75mm (D_1/D=1.07) were detected to test the detection sensitivity of Helmholtz probe to the pipe radius. The axial cracks with the depth in the range of 2 to 10 mm were machined in the pipe by EDM, as shown in Figure.19.

The pipe were moved along the axial direction at a speed of 10mm/s and the B_z signals were measured and shown in Figure.20. From the figures we can see that all of the cracks in pipe could be detected obviously. The background magnetic field signal of ϕ 65 pipe is about 30% bigger than that of ϕ 75 pipe, which is caused by the amplifier in hardware. Moreover, the sensitivity of B_z signals were calculated and shown in Figure.21. It is apparent from this figure that the sensitivity of B_z of the ϕ 65 and ϕ 75 pipes are almost the same and the sensitivity of B_z signal increases with the increasing of crack depth, which means that the Helmholtz probe has prospect in crack sizing. The radius of pipe has little effect on detection sensitivity through the Helmholtz Probe proposed in this paper.

5 Conclusions

In this work, a Helmholtz-coil-type electromagnetic probe was presented for detection of multiple type defect in pipe. The simulation and experiment results indicated that when ferromagnetic pipe locate in the center of the Helmholtz probe excited by alternating current, magnetic field and current field will be induced in axial and circumferential directions respectively on the surface of pipe. The multiply type defects in pipe can be detected by the superposition effect of the current perturbation and the magnetic flux leakage. The profile of the defects can be recognized approximately through the sensor array. Meanwhile, the experiment result verified that the radius of pipe has little effect on the detection sensitivity through the Helmholtz probe proposed in this paper.

Although different surface defects can be detected in our research, the subsurface defects can hardly be detected. In the future work, we will focus on the subsurface defect detection. Moreover, to establish an efficient and robust detection system, some numerical algorithms will also be used in the future.

Acknowledgment

This work was funded by the National Natural Science Foundation of China (No. 51574276 and No. 51675536), the Shandong Provincial Natural Science Foundation (No.ZR2015EM009), Special national key research and development plan (No.2016YFC0802300 and No.2016YFC0303800), and the Fundamental Research Funds for the Central Universities (No.16CX06017A, No. 15CX05024A and No. 14CX02198A).

Reference

[1] Li W, Yuan X, Chen G, et al. A feed-through ACFM probe with sensor array for pipe string cracks inspection. NDT & E International, 2014, 67(8):17-23.

[2] Smith, M, and R. Sutherby. The detection of pipeline SCC flaws using the ACFM technique. Insight: Non-Destructive Testing & Condition Monitoring volume 47.12(2005):765-768

[3] Nestleroth J B, Davis R J. Application of eddy currents induced by permanent magnets for pipeline inspection. NDT & E International, 2007, 40(1):77-84.

[4] Jarvis R, Cawley P, Nagy P B. Current deflection NDE for the inspection and monitoring of pipes. NDT & E International, 2016, 81:46-59.

[5] Wu J, Sun Y, Kang Y, et al. Theoretical Analyses of MFL Signal Affected by Discontinuity Orientation and Sensor-Scanning Direction. IEEE Transactions on Magnetics, 2015, 51(1):1-7.

[6] Ireland R C, Torres C R. Finite element modelling of a circumferential magnetiser. Sensors & Actuators A Physical, 2006, 129(1–2):197-202.

[7] Katragadda G, Lord W, Sun Y S, et al. Alternative magnetic flux leakage modalities for pipeline inspection. IEEE transactions on magnetics, 1996, 32(3): 1581-1584.

[8] Gotoh Y, Takahashi N. 3-D nonlinear eddy current analysis of factors affecting the evaluation of alternating flux leakage testing. International Journal of Applied Electromagnetics and Mechanics, 2001, 14(1-4): 29-34.

[9] Shi Y, Zhang C, Li R, et al. Theory and Application of Magnetic Flux Leakage Pipeline Detection. Sensors, 2015, 15(12):31036-31055.

[10] Beller, Michael，Mastering the Inspection of Challenging Pipelines. Pipeline & Gas Journal, 2015,242(11):30-36.

[11] Mak D K. Ultrasonic methods for measuring crack location, crack height and crack angle. Ultrasonics, 1985, 23(5):223-226.

[12] Xiaoxia Y, Shili C, Shijiu J, et al. Crack orientation and depth estimation in a low-pressure

turbine disc using a phased array ultrasonic transducer and an artificial neural network. Sensors, 2013, 13(9):12375-91.

[13] Ashigwuike E C, Ushie O J, Mackay R, et al. A study of the transduction mechanisms of electromagnetic acoustic transducers (EMATs) on pipe steel materials. Sensors & Actuators A Physical, 2015, 229:154-165.

[14] Thring C B, Fan Y, Edwards R S. Focused Rayleigh wave EMAT for characterisation of surface-breaking defects. NDT & E International, 2016, 81:20-27.

[15] Xie Y, Yin W, Liu Z, et al. Simulation of ultrasonic and EMAT arrays using FEM and FDTD. Ultrasonics, 2015, 66:154-165.

[16] C. Scruby, B. Moss, Non-contact ultrasonic measurements on steel at elevated temperatures, NDT & E Int. 26 (4) (1993) 177–188.

[17] Na W B, Kundu T. A combination of PZT and EMAT transducers for interface inspection. Journal of the Acoustical Society of America, 2002, 111(1):2128-39.

[18] Qiu L, Yuan S, Bao Q, et al. Crack propagation monitoring in a full-scale aircraft fatigue test based on guided wave-Gaussian mixture model. Smart Materials & Structures, 2016, 25(5):055048.

[19] Leinov E, Lowe M J S, Cawley P. Investigation of guided wave propagation and attenuation in pipe buried in sand. Journal of Sound & Vibration, 2015, 347:96-114.

[20] Lowe M J S, Alleyne D N, Cawley P. Defect detection in pipes using guided waves. Ultrasonics, 1998, 36(1-5): 147-154.

[21] Wagner R, Goncalves O, Demma A, et al. Guided wave testing performance studies: comparison with ultrasonic and magnetic flux leakage pigs. Insight-Non-Destructive Testing and Condition Monitoring, 2013, 55(4): 187-196.

[22] Cawley P, Cegla F, Stone M. Corrosion Monitoring Strategies—Choice Between Area and Point Measurements. Journal of Nondestructive Evaluation, 2012, 32(2):156-163.

[23] Ahmad R. Guided Wave Technique to Detect Defects in Pipes Using Wavelet Analysis. University of Arizona.2005.

[24] Xu J, Xiong H, Wu X. Signal processing for the guided wave test based on the empirical mode decomposition,International Conference on Electrical and Control Engineering. IEEE, 2011:1233-1240.

[25] Nestleroth J B, Davis R J. Application of eddy currents induced by permanent magnets for pipeline inspection. NDT & E & E International, 2007, 40(1):77-84.

[26] Ammari H, Chen J, Chen Z, et al. Target detection and characterization from electromagnetic induction data. Journal De Mathématiques Pures Et Appliquées, 2014, 101(1):54-75.

[27] Ge J, Li W, Chen G, et al. New parameters for the ACFM inspection of different materials. Insight - Non-Destructive Testing and Condition Monitoring, 2016, 58(6):313-317.

[28] Lewis A M, Michael D H, Lugg M C, et al. Thin‐skin electromagnetic fields around surface‐breaking cracks in metals. Journal of applied physics, 1988, 64(8): 3777-3784.

[29] Hasanzadeh R P R, Sadeghi S H H, Ravan M, et al. A fuzzy alignment approach to sizing surface cracks by the AC field measurement technique. NDT & E International, 2011, 44(1):75-83.

[30] Muñoz J M C, Márquez F P G, Papaelias M. Railroad inspection based on ACFM employing a non-uniform B-spline approach. Mechanical Systems & Signal Processing, 2013, 40(2):605-617.

[31] Li W, Yuan X, Chen G, et al. High sensitivity rotating alternating current field measurement

for arbitrary-angle underwater cracks. NDT & E International, 2016, 79:123-131.
[32] Li W, Chen G, et al. Analysis of the inducing frequency of a U-shaped ACFM system. NDT & E International, 2011, 44(3):324-328.
[33] Li W, Chen G, Yin X, et al. Analysis of the lift-off effect of a U-shaped ACFM system. NDT & E International, 2013, 53(1):31-35.
[34] Vorob'ev A A, Dremin A N, Savvin L I, et al. Utilization of a helmholtz coil in the electromagnetic method. Combustion, Explosion, and Shock Waves, 1983, 19(4): 508-511.
[35] Trout S R. Use of Helmholtz coils for magnetic measurements. IEEE Transactions on Magnetics, 1988, 24(4):2108-2111.
[36] Peng J, Tian G Y, Wang L, et al. Investigation into eddy current pulsed thermography for rolling contact fatigue detection and characterization. NDT & E International, 2015, 26(6):2825-31.
[37] Li K, Tian G Y, Cheng L, et al. State Detection of Bond Wires in IGBT Modules Using Eddy Current Pulsed Thermography. IEEE Transactions on Power Electronics, 2014, 29(29):5000-5009.
[38] Hatsukade Y, Okuno S, Mori K, et al. Eddy-current-based SQUID-NDE for detection of surface flaws on Copper tubes. IEEE Transactions on Applied Superconductivity, 2007, 17(2):780-783.
[39] Wu B, Wang Y J, Liu X C, et al. A novel TMR-based MFL sensor for steel wire rope inspection using the orthogonal test method. Smart Materials and Structures, 2015. 24(7): p. 075007.
[40] Dodd C V, Deeds W E. Analytical Solutions to Eddy‐Current Probe‐Coil Problems. Journal of Applied Physics, 1967, 39(6):2829-2838.
[41] Dodd C V, Solutions to Electromagnetic Induction Problems Oak Ridge National Laboratory, ORNL-TM-1842 (1967), Ph.D' dissertation, the University of Tennessee, 1967.
[42] Dodd C V, Cheng C C, Deeds W E. Induction coils coaxial with an arbitrary number of cylindrical conductors. Journal of Applied Physics, 1974, 45(2):638-647.
[43] Ammari H, Kang H, Kim E, et al. A MUSIC-type algorithm for detecting internal corrosion from electrostatic boundary measurements. Numerische Mathematik, 2008, 108(4):501-528.
[44] Nicholson G L, Davis C L. Modelling of the response of an ACFM sensor to rail and rail wheel RCF cracks. NDT & E International, 2012, 46: 107-114.
[45] Gui Y T, Gao Y, Li K, et al. Eddy Current Pulsed Thermography with Different Excitation Configurations for Metallic Material and Defect Characterization. Sensors, 2016, 16(6):843.

Figure caption

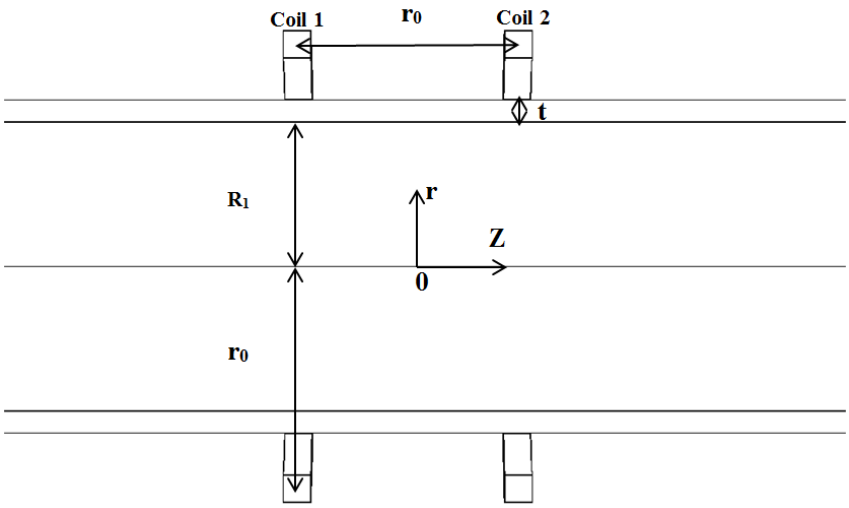

Figure.1 Helmholtz coil encircling a pipe string

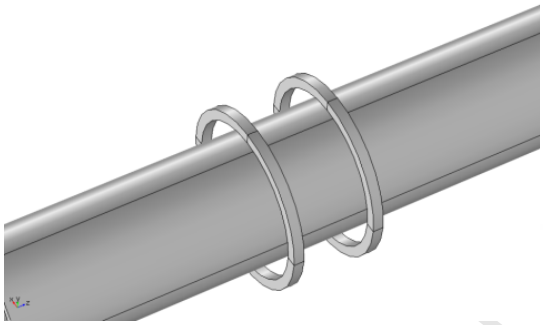

Figure.2 Finite element model of Helmholtz coil probe

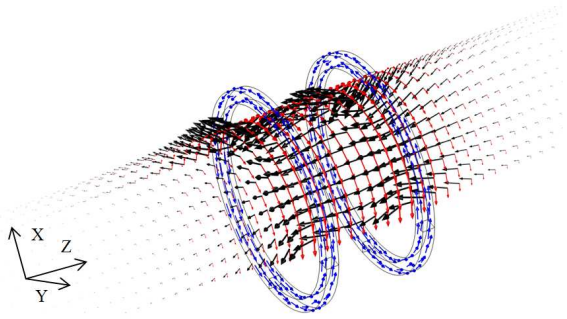

Figure.3 Induced electromagnetic field on the surface of the pipe

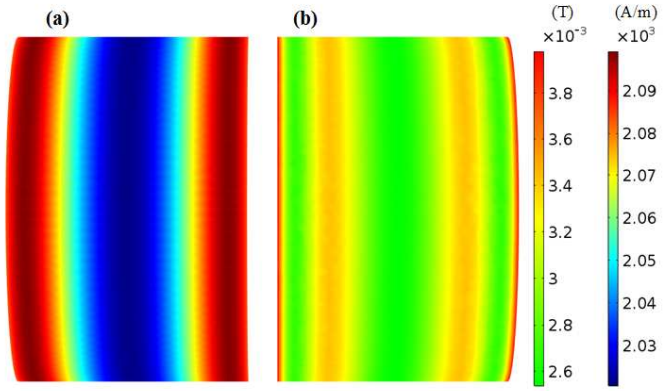

Figure.4 a)Induced electric current field and b)Induced magnetic field in pipe

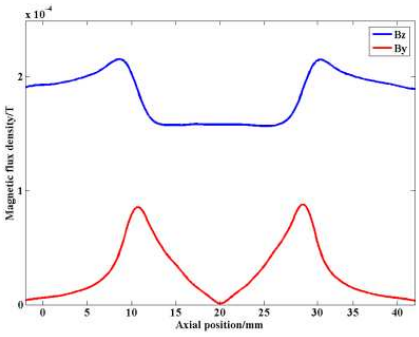

Figure.5 Axial crack signal

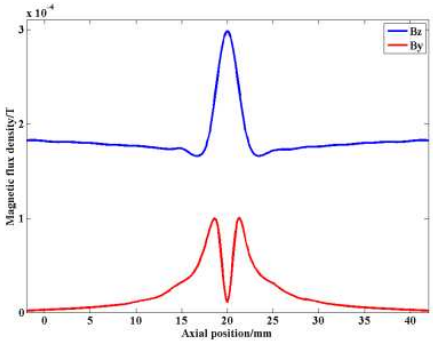

Figure.6 Circumferential crack signal

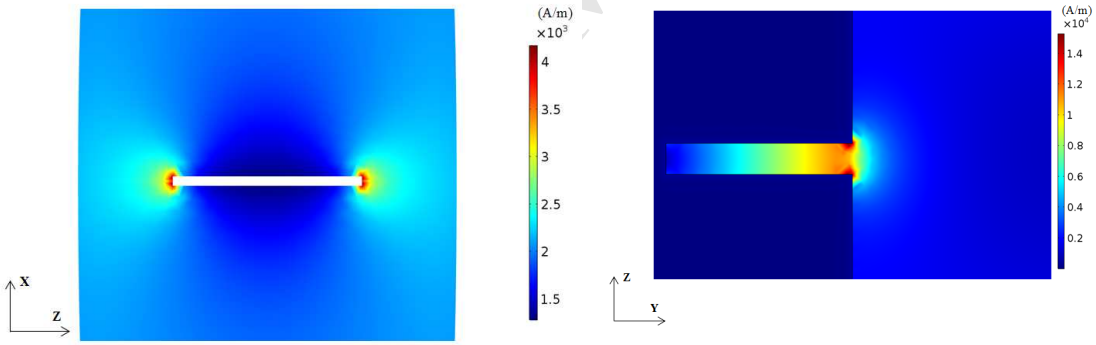

a) Current perturbation effect b) Magnetic flux leakage effect

Figure.7 Electromagnetic distortion around a) axial crack and b) circumferential crack

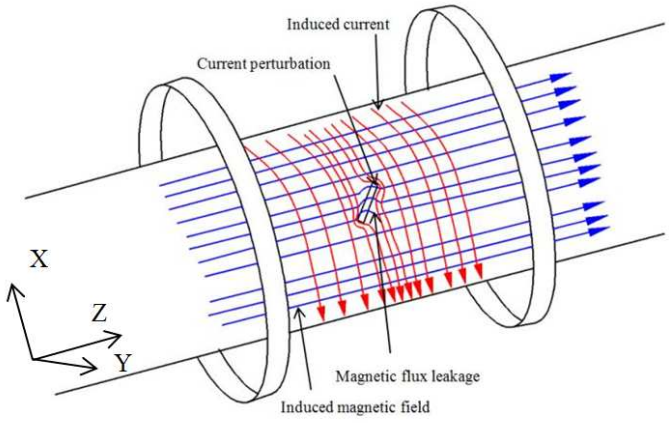

Figure.8 Current perturbation and magnetic flux leakage around defect

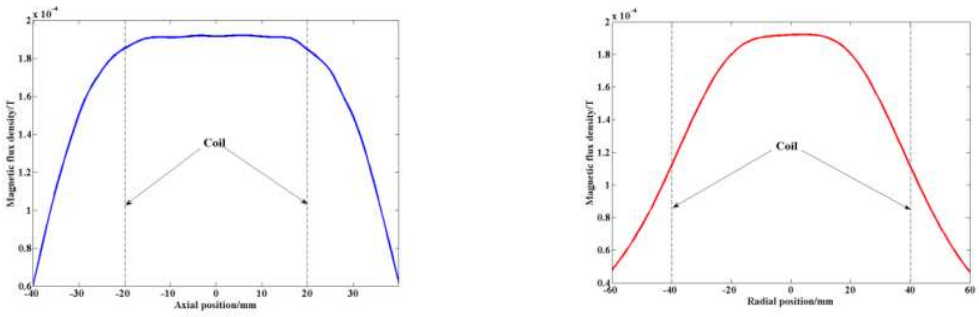

a) b)

Figure.9 Magnetic field distribution between Helmholtz coil, a) along axial direction, b) Along radial direction

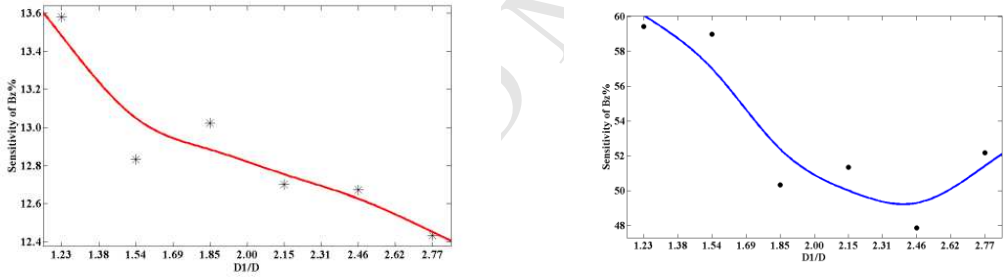

a) b)

Figure.10 Detection sensitivity of axial and circumferential cracks vs. coil radius, a) axial crack, b) circumferential cracks

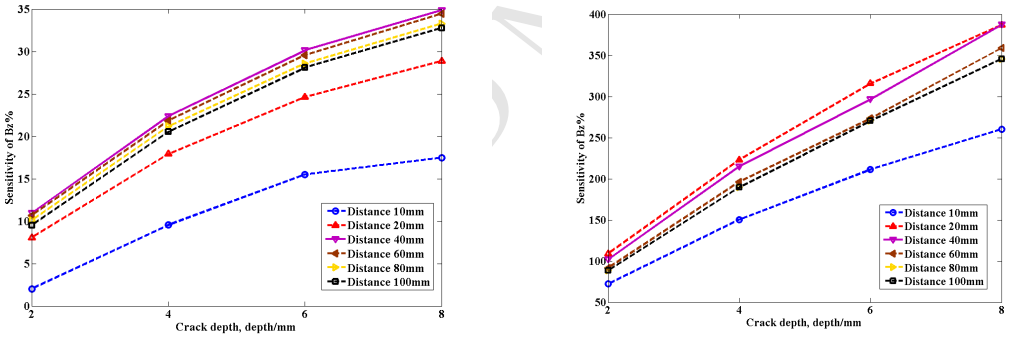

a) b)

Figure.11 Detection sensitivity vs coil distance, a)axial cracks and b)circumferential cracks

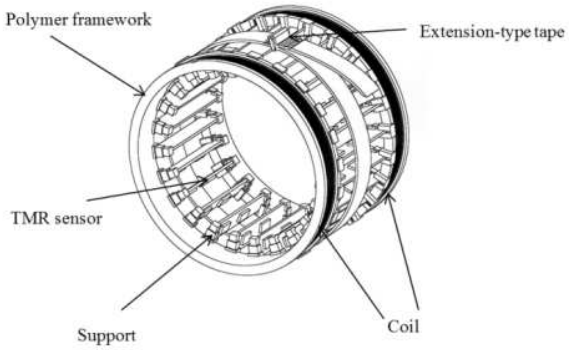

Figure.12 Structure of the Helmholtz probe

Figure.13 PCB of TMR sensor

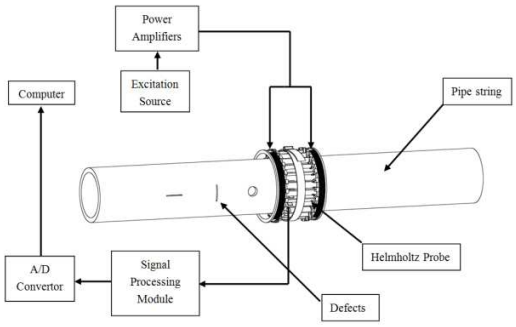

Figure.14 Structure of the Helmholtz probe electromagnetic detection system

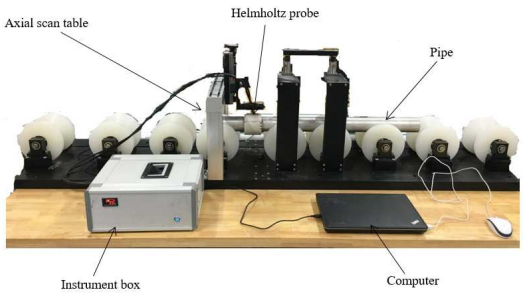

Figure.15 Experimental setup

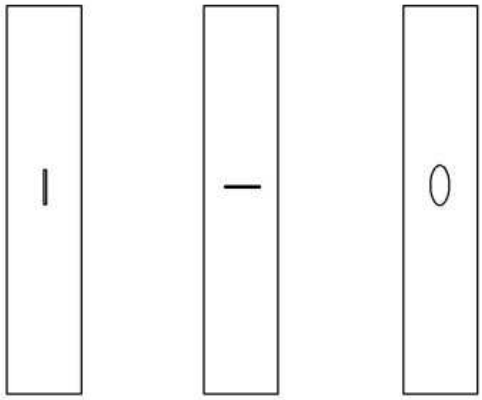

Figure.16 Defects in pipes

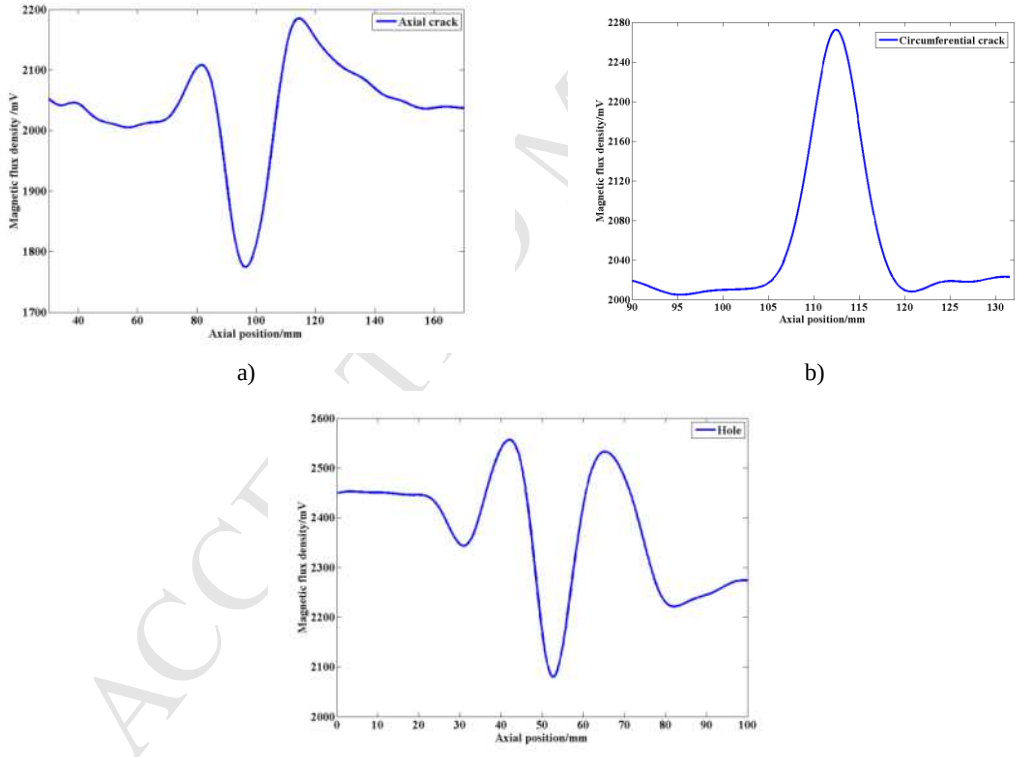

a) b)

c)

Figure.17 Bz of defects a) Axial crack, b) Circumferential crack, c) Hole

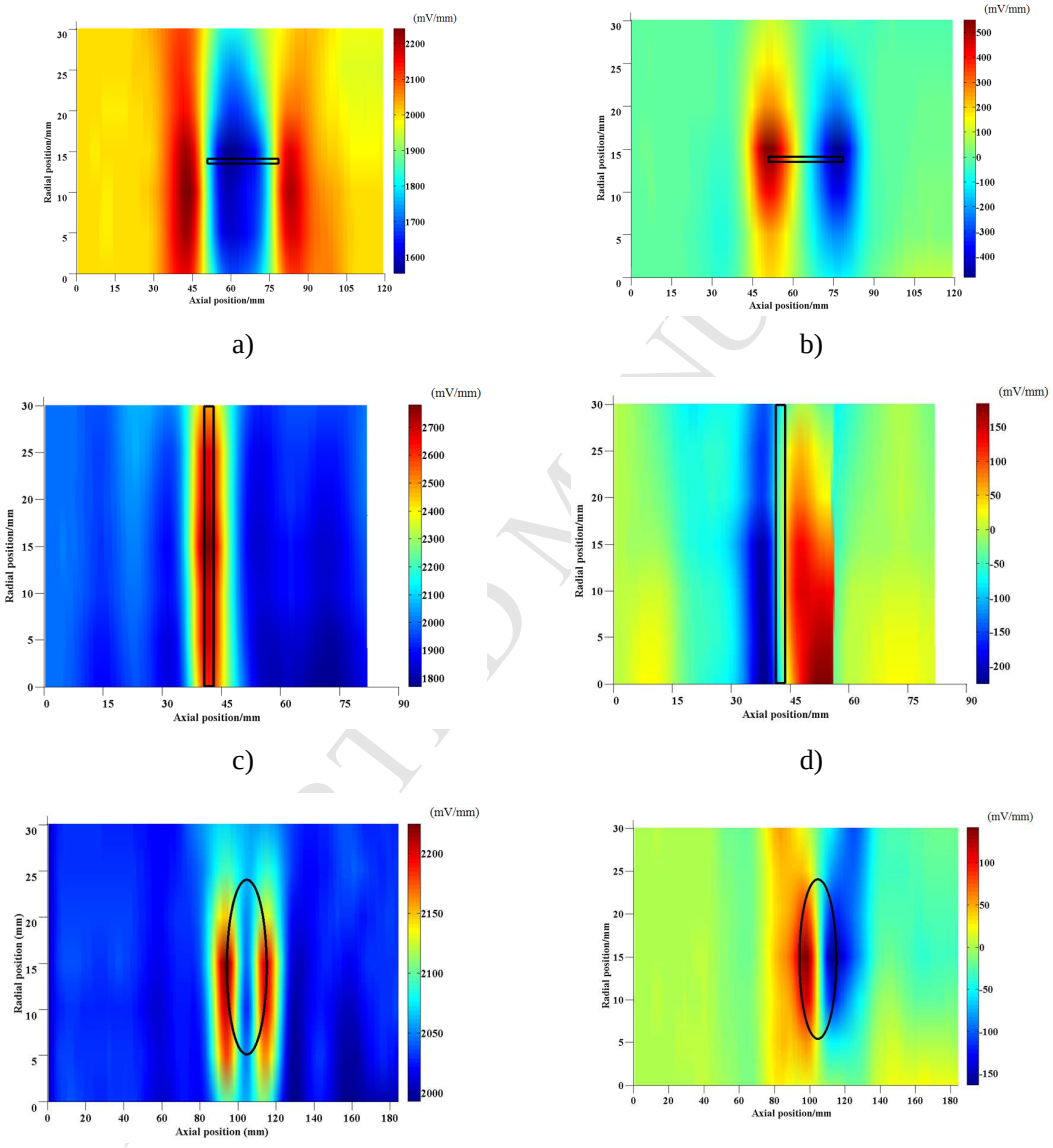

Figure.18 surface scan results, a) B_z of the axial crack, b) B_y of the Axial crack, c) B_z of the circumferential crack, d) B_y of the Circumferential crack, e) B_z of the hole, f) B_y of the hole

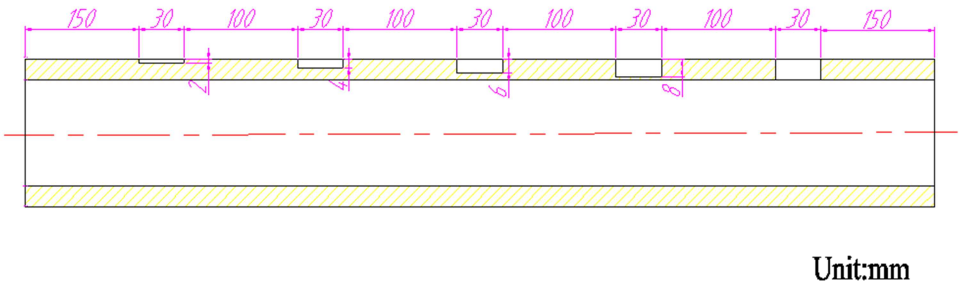

Figure.19 Axial cracks in pipe

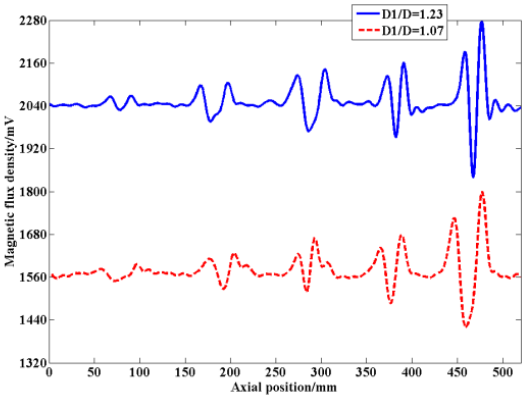

Figure.20 B_z signal of pipe

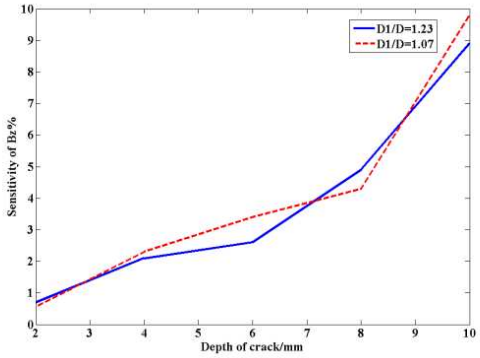

Figure.21 Sensitivity of B_z signal of pipe

1) A novel Helmholtz electromagnetic probe excited by alternating current is proposed in this paper

2) A high precision sensor array that is consisted of the (tunnel magneto-resistive) TMR is constructed.

3) By the virtue of the orthogonal uniform current field and magnetic field induced by the Helmholtz coil, various types of defects such as hole, axial crack and circumferential crack on the surface of the pipe string can be detected out.

4) The radius of pipe string has little effect on defect detection sensitivity through the Helmholtz Probe proposed in this paper.